# Combined FDOPA and 3OMFD PET Studies in Parkinson's Disease

Vijay Dhawan, Tatsuya Ishikawa, Clifford Patlak, Thomas Chaly, William Robeson, Abdelfatihe Belakhlef, Claude Margouleff, Francine Mandel and David Eidelberg

*Departments of Neurology, Research, Medicine and Biostatistics, North Shore University Hospital/Cornell University Medical College, Manhasset, New York; and State University of New York at Stony Brook, New York*

PET has been used to quantify striatal 6-[$^{18}$F]fluoro-L-dopa (FDOPA) uptake as a measure of presynaptic dopaminergic function. It has been suggested that the estimation of dopa-decarboxylation (DDC) rate, $k_3^D$, using a compartmental approach to dynamic FDOPA/PET data, can provide a better objective marker of parkinsonism. This modeling process, however, requires many assumptions to estimate DDC activity with acceptable errors. **Methods:** We combined FDOPA 3-O-methyl-fluorodopa PET studies on three normal subjects and five Parkinson's disease patients. **Results:** The contradicted modeling assumptions are: (a) the rate constants across the blood-brain barrier, $K_1^D$ and $k_2^D$, for 3OMFD and FDOPA were in similar range (ratio ≅ 1) and thus not equal to assumed values of $K_1^M/K_1^D$ of 2.3 derived from rat studies and applied to human FDOPA studies and (b) the $K_1^D/k_2^D$ ratio for frontal cortex was not equal to that for the striatum (0.70 ± 0.15 versus 1.07 ± 0.3; $p < 0.002$). Discriminant analyses indicate that simple estimates like the striatum-to-occipital ratio, or the graphically derived unidirectional transport rate constant ($K_i^{FD}$) separate normals from Parkinson's disease patients at least as accurately as estimates of striatal DDC activity ($k_3^D$). **Conclusion:** Measurements of striatal DDC activity with dynamic FDOPA/PET and compartmental modeling may be based on incorrect assumptions. Even though such complex models yield microparameters that may be applicable to certain clinical research demands, they may produce misleading results in other experimental settings.

**Key Words:** PET; compartmental modeling; Parkinson's disease; nigrostriatal dopaminergic function; F-DOPA; 3OMFD

**J Nucl Med 1996; 37:209–216**

6-[$^{18}$F]fluoro-L-dopa (FDOPA) has been used with quantitative PET to assess presynaptic nigrostriatal dopaminergic function in life. To be clinically useful, FDOPA/PET must yield quantitative parameters that correlate closely with independent disease severity measures and discriminate reliably between patients with mild early disease, or with preclinical involvement, and normal control subjects.

A variety of compartmental models have been developed to quantitate FDOPA/PET images for these purposes. The differences in these models arise because different sets of assumptions are made in each case and the ultimate number of parameters are estimated (*1–4*). We have analyzed the model shown in Figure 1. The metabolites FDA (fluorodopamine) and FMT (3-methoxy-6-[$^{18}$F]fluorotyramine) are considered to be nondiffusible metabolites, whereas FDOPAC (L-3,4-dihydroxy-6-[$^{18}$F]fluorophenylacetic acid) and FHVA (6-[$^{18}$F]fluorohomovalinic) are considered diffusible metabolites. The rate constant $k_7^D$ represents the conversion of FDA to FDOPAC and FHVA and $k_9^D$ is the rate of loss of diffusible metabolites. A very small amount of O-methylation of FDOPA to OMFD in brain is shown by the rate constant $k_5^D$. The parameter of physiological significance in Parkinson's disease has been postulated to be the dopa decarboxylase step in the metabolism of DOPA to dopamine (DA) (*4*). This step is defined by the rate constant $k_3^D$ and is thought to be more sensitive to presynaptic nigrostriatal dopaminergic process in Parkinson's disease than the the unidirectional transfer constant $K_i^{FD}$, estimated from multiple time graphical approach (MTGA) (*5*), which also includes the capillary exchange process.

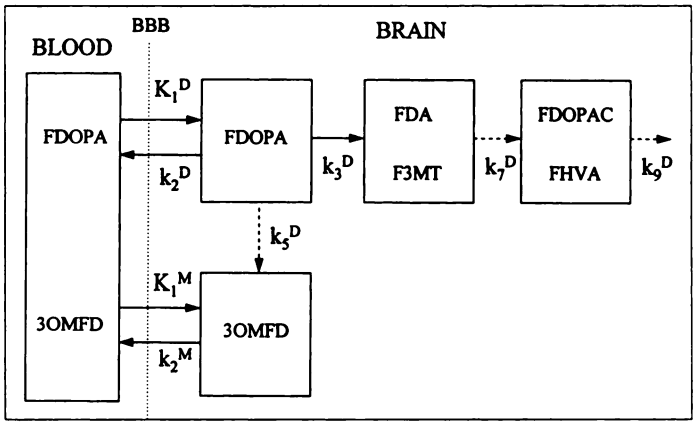


**FIGURE 1.** Compartmental model for the biodistribution of FDOPA previously published by Kuwabara et al. (*4*). The nomenclature was retained for comparison purposes. The rate constants shown (dotted line) emphasize the marginal contribution of these processes for a 100-min study.

To address this issue, we used PET to study subjects with FDOPA and with 3OMFD, a metabolite of FDOPA which crosses the blood-brain barrier but is not significantly trapped in brain tissue. We examined the mathematical and physiological correlates of the parameters estimated according to each of the various compartmental approaches.

## MATERIALS AND METHODS

### Normal Subjects

We studied three normal volunteer subjects (1 man, 2 women; mean age, 22 ± 4 yr). The exclusion criteria used were past history of neurological or psychiatric illness; prior exposure to neuroleptic agents or drug use; past medical history of hypertension, cardiovascular disease and diabetes mellitus and abnormal neurological examination.

### Patients with Parkinson's Disease

We studied five classical Parkinson's disease patients without dementia (2 men, 3 women; age 63 ± 14 yr). This group was selected with mild/moderate clinical involvement (Hoehn and Yahr Stages I–III (*6*); see Table 1). Ethical permission for these studies was obtained from the Institutional Review Board of North Shore University Hospital/Cornell University Medical College. Written consent for all subjects was obtained following a detailed explanation of the scanning procedure.

Received Nov. 28, 1994; revision accepted Jun. 26, 1995.

For correspondence or reprints contact: Vijay Dhawan, PhD, Department of Neurology North Shore University Hospital/Cornell University Medical College, 300 Community Drive, Manhasset, NY 11030.

**TABLE 1**
Clinical Summary: Parkinson's Disease Patients

| Patient no. | Age (yr) | Sex | H&Y | Drugs* | Tremor | Rigidity | Gait | AI† | UPDRS |
|---|---|---|---|---|---|---|---|---|---|
| 1 | 77 | M | I | 1 | 4 | 1 | 0 | 5 | 9 |
| 2 | 72 | M | I | 2, 3 | 4 | 5 | 0 | −7 | 15 |
| 3 | 57 | F | II | 1 | 0 | 1 | 0 | 4 | 10 |
| 4 | 42 | F | II | 2, 3 | 4 | 4 | 0 | 0 | 12 |
| 5 | 66 | F | III | 1, 2 | 3 | 3 | 2 | 1 | 21 |

*Drugs: 1 = levodopa/carbidopa, 2 = deprenyl, 3 = anticholinergics.
†Asymmetry index calculated by subtracting the left UPDRS scores from the right scores. Positive AI reflects higher clinical involvement of the right body side.
UPDRS = Unified Parkinson Disease Rating Scale composite scores (UPDRS 3.0; items 19–31), H&Y = Hoehn and Yahr stage

## PET

All subjects fasted overnight prior to PET scanning. All antiparkinsonian medications were discontinued at least 12 hr before PET investigations. At the time of the PET study all Parkinson's disease patients were rated quantitatively according to the Hoehn and Yahr Scale and the Unified Parkinson Disease Rating Scale (UPDRS 3.0) (*7*). PET studies were performed using the Superpett 3000 tomograph (Scanditronix; Essex, MA). The performance characteristics of this instrument have been described elsewhere (*8*). This four ring $BaF_2$ time-of-flight, whole-body tomograph acquires 14 PET slices with z-axis gantry translation. Each slice is 8 mm thick and is reconstructed with an in-plane resolution of 7.5 mm (FWHM) in high resolution mode.

Subjects were positioned in the scanner in a stereotaxic head holder with three-dimensional laser alignment (*9*). All studies were performed with the eyes open in a dimly-lit room with minimal auditory stimulation. FDOPA was produced according to the radiochemical synthesis of Luxen (*10*) and was >95% radiochemically pure (specific activity approximately 15 MBq/μmole). All subjects received 200 mg carbidopa 1.5 hr before the study to inhibit decarboxylation (*11*). A total of 185–370 MBq FDOPA in 20–25 ml saline was injected into an antecubital vein over 45 sec with an automated infusion pump. Emission scanning began simultaneously with the start of the FDOPA injection, and continuous scan data were acquired in list mode between 0 and 100 min postinjection. PET images were reconstructed with a correction for measured tissue attenuation and for random coincidences, electronic dead time and scatter effects.

The time course of plasma $^{18}F$ radioactivity was determined by radial arterial blood sampling followed by plasma centrifugation. Sixteen 9 sec samples were taken by a precision peristaltic pump followed by nine discrete samples taken over the next 100 min postinjection. Because the first 16 arterial samples were collected using a pump, an appropriate smearing correction was applied (*12*). In the six blood samples taken at 10, 25, 40, 55, 70 and 85 min postinjection, plasma FDOPA was separated from its metabolites using HPLC with radiochemical detection. The details of the HPLC analysis have been described elsewhere (*13*).

The procedure for the 3OMFD/PET study was exactly the same as the one for FDOPA described above, except no carbidopa was administered. The radiochemical purity of 3OMFD was >98% and the specific activity was estimated to be approximately 11,000 MBq/mmole (*14*). All subjects received 185–370 MBq 3OMFD intravenously in a fashion identical to the FDOPA studies described above. The time interval between FDOPA and 3OMFD on the same subject varied from 1 day to 4 wk. The sterotaxic headholder allowed us to reposition the subject to within 2 mm of the first study (*9*).

## Image Analysis

Region of interest (ROI) analysis was performed on 128 × 128 PET reconstructions using a SUN microcomputer and Scan/VP Software (*15*). Striatal and occipital ROIs were identified by visual inspection with reference to a standard neuroanatomical atlas (*16*). Elliptical ROIs were placed interactively on composite (40–100 min) PET brain slices to outline the whole striatum (mean 90 pixels/striatum; pixel size 4 $mm^2$). These ROIs were transferred to the 3OMFD images that were prealigned with the FDOPA images because the striatum was not clearly visualized in the 3OMFD scan. Irregular occipital ROIs (16–20 $cm^2$) were defined on the first 10-min scan (0–10 min) to avoid sampling activity in the transverse sinuses and torcula. Occipital count rates were assumed to represent background activity referable to nonspecific FDOPA uptake in extrastriatal tissues and to untrapped metabolites. For the graphical analysis, occipital activity concentrations were subtracted from striatal $^{18}F$-activity concentrations measured in each of six 10-min scans acquired between 40 and 100 min postinjection to obtain the time profile for specific striatal activity for FDOPA, i.e., counts referable to trapped FDOPA, $^{18}F$-fluorodopamine (FDA) and its metabolites.

Kinetic measures of FDOPA uptake were calculated by MTGA (*5*) using the time course of striatal radioactivity from 40 to 100 min postinjection and the plasma FDOPA input function. Striatal $K_i$ values calculated in this way were designated $K_i^{FD}$. In all patient and control scans, we additionally calculated the striatal-to-occipital activity ratio (SOR) by dividing striatal count rate by occipital count rate measured on the last 10-min scan taken at 90–100 min postinjection.

## Compartmental Analysis

*3OMFD Study.* The biodistribution of 3OMFD is considered primarily a facilitated diffusion process similar to the transport of L-DOPA (large neutral amino acid transport) across the blood-brain barrier (*17,18*). As there is no irreversible trapping of 3OMFD in brain tissue, the only parameters that are estimated from the kinetic data are $K_1^M$, $k_2^M$ and $V_b$.

*FDOPA Study.* The biodistribution of FDOPA is region dependent. Occipital and frontal regions have a small irreversible trapping compared to the striatal regions (*19*). The trapping of FDA is assumed to be complete during the course of the study, but the FDA undergoes further metabolism into FDOPAC and FHVA, which are back-diffusible into the plasma compartment (*11,19*).

To account for these tracer distributions, various models of increasing complexity have been applied to answer the following questions (Fig. 1):

1. Does the model need to take into account dopamine metabolism into diffusible and nondiffusible compartments (i.e., the presence of $k_7^D$, $k_9^D$)?
2. Does the model need to take into account the conversion of FDOPA to 3OMFD in the brain (i.e., the presence of $k_5^D$)?
3. Can a mathematically justifiable model which completely neglects the presence of 3OMFD (i.e., $K_1^M$ and $k_2^M$ set to zero) be justified?
4. Can frontal region $V_e^D$ (volume of distribution of FDOPA or $K_1^D/k_2^D$ ratio) be used for the striatal regions?
5. Can the $K_1^M/K_1^D$ ratio of 2.3 determined from rat studies (*20*) be used for human studies?
6. Is $k_3^D$ better than $K_i^{FD}$ at discriminating subject groups and correlating with disease severity?

Various models of increasing complexity (3–7 parameters) were tried, with and without $k_3^D$ (for frontal and occipital only), and

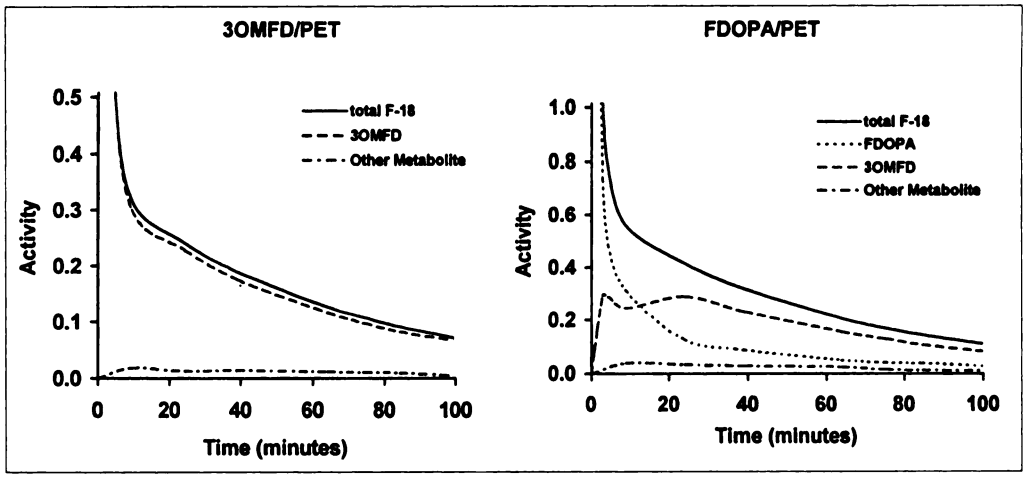


**FIGURE 2.** Arterial blood curves. 3OMFD study (left), plasma time-radioactivity curves (TACs) for $^{18}F$, 3OMFD and sulfate conjugate of FDOPAC or FHVA. The smoothed curves through the experimental data points are shown and the peak has been omitted to enhance the separation of total $^{18}F$ from the 3OMFD fraction and other metabolites at later time points. Similar TACs for the FDOPA study (right).

with: (i) $K_1^M$ and $k_2^M$ were fixed to values obtained from 3OMFD study, or (ii) allowed as independent parameters to be estimated. The model fitting was done using a nonlinear regression algorithm in PCNONLIN (Lexington, KY). The models were evaluated for bias using the residual plots, and goodness-of-fit using weighted sum-of-squares (WSS). The models were compared using the F-test as well as AIC scores (Akaike Information Criteria defined as N log(WSS) + 2p, where N is the number of observations and p is the number of parameters) (*21*).

A direct comparison of our proposed 4-parameter ($K_1^D$, $k_2^D$, $k_3^D$ and $V_b$) model M1, in which $K_1^M$ and $k_2^M$ are fixed to the values obtained from 3OMFD studies, was made with the Montreal Neurological Institute model M2, (*2*) and the McMaster University model 'M3' (*3*). The parameter $V_b$ refers to the blood volume in the ROI. The model M2 estimates three parameters ($K_1^D$, $k_3^D$ and $V_b$) while fixing the value of striatal $V_e^D$ to that obtained from a frontal region and assuming $K_1^M/K_1^D = k_2^M/k_2^D = 2.3$ based on data from rat experiments; the values of $k_7^D$ and $k_9^D$ were obtained empirically from the least normalized residual sum of squares criteria and $k_5^D$ was neglected. The model M3 is based upon the mathematically justifiable approach in which the least number of parameters ($K_1$, $k_2$ and $k_3$) that yield an optimum fit to the data are employed. The UCLA model (M2') (*1*) is a four parameter variant ($K_1^D$, $k_2^D$, $k_3^D$ and $k_4^D$ are estimated, $K_1^M/k_2^M$ is assumed to be 1.0 and $K_1^M/K_1^D$ is fixed at 1.7) of the M2 model in which $k_5^D$ and $k_9^D$ are set to zero and $k_7^D$ is defined as $k_4^D$. The mathematical treatment of these models has been published extensively and will not be duplicated here (*1–5,22–23*).

### Statistical Analysis

The following statistical procedures were performed using SAS (SAS Institute; Cary, NC):

1. Mean striatal $K_1^M$, $k_2^M$, $V_e^M$, $V_b$, $K_i^{FD}$, $k_3^D$, $K^D$ ($= K_1^D k_3^D/k_2^D + k_3^D$) and SOR values for the Parkinson's disease group were compared with analogous control values using Student's t-test.
2. Between-group discrimination for each of the parameters was assessed using a stepwise procedure with the F-test associated with Wilk's lambda (*24*). In this analysis, ipsi- and contra- striatal measures for the Parkinson's disease patients were considered independently and compared with mean right and left striatal values measured for the normal volunteers (*25*).
3. We correlated $K_i^{FD}$ with $k_3^D$(M1), $k_3^D$(M2), $k_3^D$(M3), $K_1^D$, $K^D$ and SOR for all subjects using Pearson product-moment correlation coefficients. Because of the small number of subjects, the statistical results presented here should be considered preliminary.

## RESULTS

### Plasma Analysis

The time-activity curves for FDOPA and 3OMFD were very similar for both normals and Parkinson's disease patients (Fig. 2). The breakdown function (relationship of FDOPA to total $^{18}F$ in plasma) could be modeled by a sum of two exponentials with rate constants of 0.71 ± 0.12 and 0.09 ± 0.02 $min^{-1}$ for both groups. 3OMFD had negligible breakdown over the duration of

**TABLE 2**
3OMFD Parameters Derived Using a Two-Compartment Model with Three Parameters ($K_1^M$, $k_2^M$ and $V_b$)

| | $K_1^M$ | $k_2^M$ | $V_b$ | $V_e^M$ |
|---|---|---|---|---|
| Normal (n = 3) | | | | |
| Frontal | 0.027 ± 0.003 | 0.039 ± 0.002 | 0.026 ± 0.016 | 0.701 ± 0.038 |
| Occipital | 0.033 ± 0.002 | 0.049 ± 0.006 | 0.032 ± 0.017 | 0.677 ± 0.104 |
| Striatum | 0.029 ± 0.003* | 0.036 ± 0.006 | 0.029 ± 0.017 | 0.815 ± 0.139 |
| PD (n = 5) | | | | |
| Frontal | 0.043 ± 0.011 | 0.052 ± 0.020 | 0.030 ± 0.007 | 0.872 ± 0.219 |
| Occipital | 0.057 ± 0.018 | 0.065 ± 0.021 | 0.047 ± 0.023 | 0.897 ± 0.239 |
| L. striatum | 0.047 ± 0.013* | 0.046 ± 0.015 | 0.039 ± 0.006 | 1.049 ± 0.241 |
| R. striatum | 0.047 ± 0.015* | 0.046 ± 0.016 | 0.035 ± 0.011 | 1.041 ± 0.215 |

*Significant difference between normal from PD groups ($p < 0.048$).
All table entries are mean ± s.d.
PD = Parkinson's disease; $V_e^M = K_1^M/k_2^M$; $K_1^M$ and $k_2^M$ are expressed as ml/min/g and $min^{-1}$, respectively.

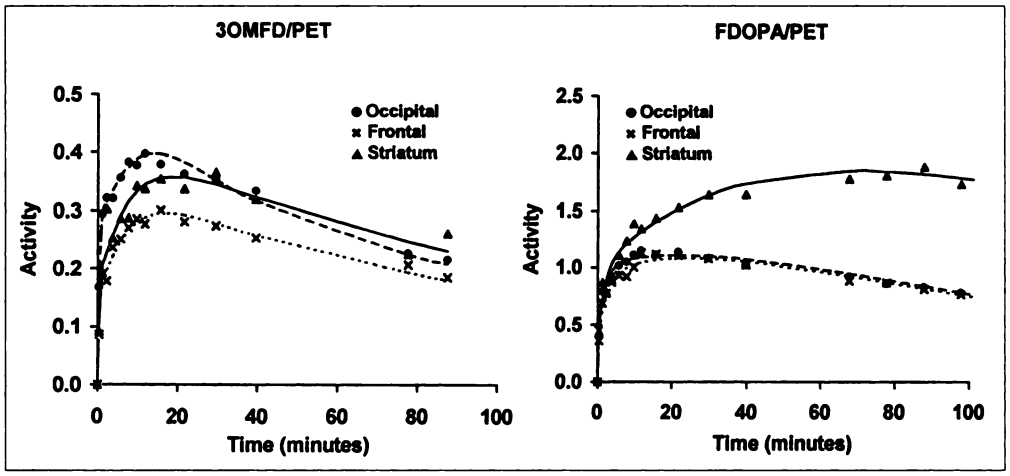


**FIGURE 3.** Brain curves. 3OMFD study (left). Time-radioactivity curves (TACs) showing the striatum, frontal and occipital cortex in the same subject. The two-compartment, three-parameter model fitted curves are superimposed on the data points (see text). Similar TACs for the FDOPA study (right): the fitted curves from model 'M1' are superimposed.

the study with <5% of unknown metabolite (Fig. 2A). This fraction was thought to represent a sulfate conjugate (*26*). The 3OMFD results are presented in Table 2 and Figure 3A.

Good model fits were obtained with no bias and standard error of estimate (s.e.e) of parameters are <15% for $K_1^M$ and $k_2^M$ and <30% for $V_b$. There was no statistical difference between $V_e^M$ for striatum and frontal ROIs ($p > 0.1$) for both the normal and Parkinson's disease groups. Normal subjects have a lower mean striatum $K_1^M$ as compared to the Parkinson's disease group (0.029 ± 0.003 versus 0.047 ± 0.014; $p = 0.048$; see Fig. 4). Even though the mean values of $k_2^M$ and $V_b$ are 15%–25% lower for normal subjects than Parkinson's disease patients, these differences are not statistically significant.

*FDOPA.* All results below are from model M1 unless specified.

*Frontal and Occipital.* The results are presented in Table 3 and Figures 3B and 5. The dopa decarboxylase rate constant, $k_3^D$, was found to be essential for obtaining a good fit (6 out of 8 subjects showed a significant decrease of bias and weighted sum-of-squares). The partition volume for DOPA, $V_e^D$, was significantly different for frontal cortex and occipital regions ($p < 0.002$). No differences were found in $V_e^D$ for normals and Parkinson's disease patients ($p > 0.1$). Mean $k_3^D$ was 40% lower in the Parkinson's disease group compared to normal (Table 3) but was not statistically significant. The model M2 yields a higher $k_3^D$ than our model, 0.0105 ± 0.0061 versus 0.0035 ± 0.0043 ($N = 8$, $p < 0.002$). If a floating 'q' parameter ($K_1^M/K_1^D = k_2^M/k_2^D$) was fitted (in addition to $K_1^D$, $k_2^D$, $k_3^D$ and $V_b$ for a total of 5 parameters) instead of using 3OMFD/PET-derived measures of $K_1^M$ and $k_2^M$, we found that estimated q values for frontal ranged from 0.8–3.0 (1.93 ± 0.84). The goodness-of-fit criteria suggest that model M2 and the 5-parameter model (M1 with a floating q) were similar to the 4-parameter model M1.

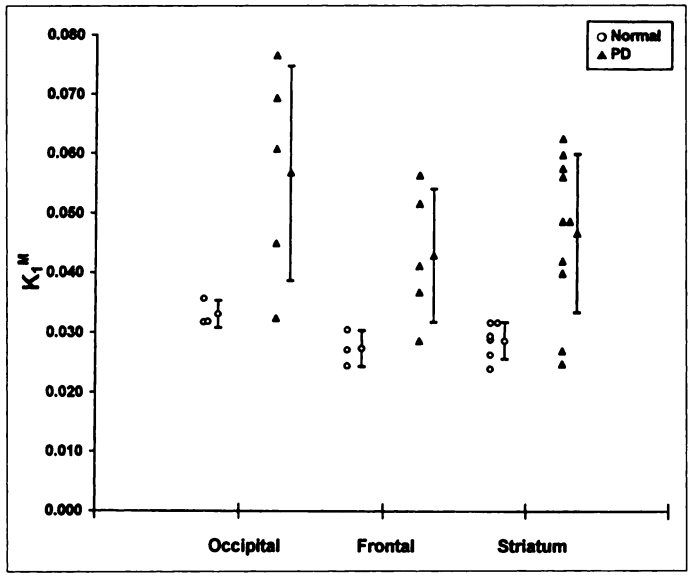


**FIGURE 4.** $K_1^M$ values derived from a two-compartment, three-parameter model ($K_1^M$, $k_2^M$ and $V_e^M$ estimated) for normal controls and Parkinson's disease (PD) patients.

### Striatum

Results are presented in Table 4 and Figures 5, 6 and 7.

*Q.1 & Q.2.* Similar fits were obtained with and without $k_5^D$, $k_7^D$ and $k_9^D$ as judged by the bias and F test on WSS ($p > 0.2$). The parameter $k_3^D$, obtained by neglecting $k_5^D$, $k_7^D$ and $k_9^D$, correlated perfectly when population values of $k_5^D$, $k_7^D$ and $k_9^D$ (0.001, 0.01, 0.002 respectively) were utilized ($r = 0.99$, $p < 0.0001$).

*Q.3.* Similar fits (by WSS criteria) were observed when $K_1^M$ and $k_2^M$ were neglected (total $^{18}F$ plasma input function was used instead of plasma FDOPA time-activity curve).

*Q.4.* The parameter $V_e^D$ for frontal cortex is 20%–30% lower than for striatum ($p < 0.002$).

*Q.5.* The parameters $K_1^D$ and $k_2^D$ had a range similar to $K_1^M$ and $k_2^M$ (Table 2 and 3) with $K_1^M/k_2^M \cong 1.0$ for both normal and Parkinson's disease groups across all regions.

*Q.6.* The graphical influx constant $K_i^{FD}$ separates the groups marginally better than $k_3^D$ ($F[1, 6] = 18.8$, $p = 0.005$ and $F[1, 6] = 11.9$, $p = 0.014$, respectively).

Discriminant analysis indicated that SOR distinguished Parkinson's disease patients from normals more accurately than the other parameters ($F[1, 6] = 46.7$, $p = 0.0005$). SOR correctly classified all normals and Parkinson's disease patients. $K_i^{FD}$ discriminated Parkinson's disease patients from normals as accurately as SOR. Estimates of $k_3^D$(M1), $k_3^D$(M2) and $k_3^D$(M3) discriminated between the two groups but not as accurately as $K_i^{FD}$ and SOR. Correlation analysis revealed $K_i^{FD}$ to be significantly correlated with the other parameters ($r = 0.97$, 0.91 and 0.95 for $K_i^{FD}$ correlations with $k_3^D$, $K^D$, and SOR, respectively; $p < 0.0001$ for all correlations; Fig. 7).

## DISCUSSION

### Plasma Analysis

Our results suggest that the peripheral FDOPA breakdown is similar in normals and Parkinson's disease patients. Addition-

**TABLE 3**
FDOPA Model 'M1' Estimated Parameters ($K_1^D$, $k_2^D$, $k_3^D$ and $V_b$) for Frontal, Occipital and Striatum*

| | $K_1^D$ | $k_2^D$ | $k_3^D$ | $V_b$ | $V_e^D$ |
|---|---|---|---|---|---|
| Normal (n = 3) | | | | | |
| Frontal | 0.039 ± 0.007 | 0.056 ± 0.004 | 0.005 ± 0.003 | 0.014 ± 0.005 | 0.696 ± 0.189 |
| Occipital | 0.050 ± 0.011 | 0.064 ± 0.007 | 0.004 ± 0.002 | 0.024 ± 0.009 | 0.791 ± 0.259 |
| Striatum | 0.042 ± 0.007 | 0.038 ± 0.008 | 0.024 ± 0.011* | 0.019 ± 0.006 | 1.178 ± 0.414 |
| PD (n = 5) | | | | | |
| Frontal | 0.041 ± 0.005 | 0.060 ± 0.013 | 0.003 ± 0.005 | 0.030 ± 0.007 | 0.707 ± 0.149 |
| Occipital | 0.055 ± 0.013 | 0.070 ± 0.012 | 0.002 ± 0.003 | 0.025 ± 0.017 | 0.788 ± 0.190 |
| L. striatum | 0.045 ± 0.012 | 0.048 ± 0.013 | 0.007 ± 0.005† | 0.035 ± 0.010 | 0.952 ± 0.196 |
| R. striatum | 0.044 ± 0.010 | 0.042 ± 0.010 | 0.006 ± 0.005† | 0.036 ± 0.021 | 1.063 ± 0.239 |

*$V_e^D$ is a calculated parameter ($K_1^D/k_2^D$).
†Significant difference between normal from PD groups ($p < 0.015$)
All table entries are mean ± s.d.
PD = Parkinson's disease; $V_e^D = K_1^D/k_2^D$; $k_2^D$ and $k_3^D$ are expressed as liter/min and $K_1^D$ as ml/min/g; M1 is the four-compartment FDOPA model described in the text.

ally, peripheral 3OMFD breakdown is minimal in both groups of subjects.

## 3OMFD

The rate constants $K_1^M$ and $k_2^M$ from our 3OMFD study are similar to those measured by Doudet et al. for primates (*17*) and by Wahl et al. for humans (*18*). The known biodistribution of 3OMFD and the reasonable two-compartment model fit suggest that there is no need for a more complex model.

We find that the normal subjects have a lower $K_1^M$, $k_2^M$ and $V_e^M$ as compared to the Parkinson's disease group. Based on our previous data from fasting subjects, it is unlikely that competion with plasma amino acid levels could have played a role in this observation (*27*). The medications for Parkinson's disease subjects were discontinued at least twelve hours before the study but slow biological clearance of these drugs may play an unpredictable role. The distribution of 3OMFD is nearly uniform for all structures in the brain, although the striatum was only faintly outlined in some of the images. The kinetic differences in various regions are evident in Figure 3, where it can be seen that frontal activity is lower than that in the occipital and striatum. Our data suggest a slightly higher partition volume, $V_e^M$, for the striatum as compared to the occipital and frontal regions. These parameter values are very similar to those for [$^{11}$C]aminocyclohexanecarboxylate (ACHC), a nonmetabolized amino acid (*28*), which suggests that 3OMFD is not metabolized in the brain to any significant degree during the PET study.

## FDOPA

*Frontal and Occipital: Is $k_3^D$ Essential to These Regions?* There are independent data to suggest minimal FDOPA incorporation into cortical neurons in these regions, and the improved model fits support this (*19*). When experimentally derived 3OMFD values of $K_1^M$ and $k_2^M$ were used in our model, the estimated values of $K_1^D$ and $k_2^D$ were very similar to the corresponding 3OMFD parameters yielding a q value of approximately 1.0. When q was fitted as an additional parameter, however, its estimated value of 1.9 came close to that assumed in models M2 (q = 2.3) and M2′ (q = 1.7). The significance of this larger q value remains elusive. Even though the model M2 and a 5-parameter model (M1 with q as an additional floating parameter) resulted in similar mathematical fits, the values for 3OMFD parameters $K_1^M$ and $k_2^M$ were higher than those measured directly, and therefore were not accepted.

The partition volume, $V_e^D$, for frontal cortex is similar for models M1 and M2, 0.70 ± 0.15 vs. 0.62 ± 0.14 respectively, suggesting that the absolute values of 3OMFD parameters does not play any significant role in the estimation of $V_e^D$. The estimation of $k_3^D$, however, is very sensitive to the values of 3OMFD parameters used and needs to be taken into account for the interpretation of frontal dopa decarboxylase activity.

**TABLE 4**
Comparison of FDOPA Parameters from Compartmental Model 'M1' ($k_3^D$ and $K^D$), Multiple Time Graphical Approach ($K_i^{FD}$) and Striato-Occipital Ratio (SOR) Calculated from a Ten-Minute Scan Starting 90 Minutes Postinjection

| | $k_3^D$ | $K_i^{FD}$ | $K^D$ | SOR |
|---|---|---|---|---|
| Normal (n = 3) | | | | |
| L. striatum | 0.019 ± 0.007* | 0.015 ± 0.004† | 0.016 ± 0.007‡ | 2.24 ± 0.24§ |
| R. striatum | 0.028 ± 0.014 | 0.016 ± 0.005 | 0.016 ± 0.005 | 2.37 ± 0.15 |
| PD (n = 5) | | | | |
| L. striatum | 0.007 ± 0.005 | 0.007 ± 0.002 | 0.006 ± 0.004 | 1.51 ± 0.08 |
| R. striatum | 0.006 ± 0.005 | 0.007 ± 0.002 | 0.006 ± 0.005 | 1.58 ± 0.17 |

*†‡§Significant differences between the mean striatal values for normals and individual left and right striatal values for the PD group at $p < 0.015$, $p < 0.006$, $p < 0.039$ and $p < 0.0006$, respectively.
All table entries are mean ± s.d.
PD = Parkinson's disease; SOR = striato-occipital ratio; $K^D = K_1^D k_3^D/k_2^D + k_3^D$; $k_3^D$ and $K^D$ are expressed as $min^{-1}$ and $K_i^{FD}$ as ml/min/g; M1 is the four-compartment FDOPA model described in the text.

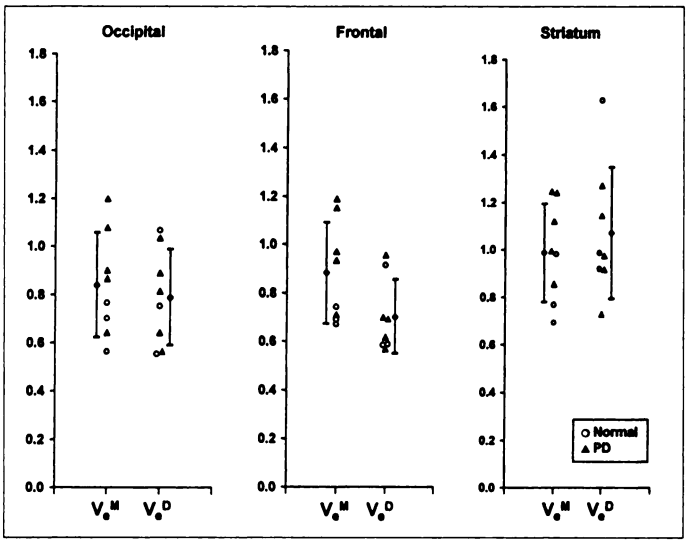


**FIGURE 5.** $V_e^M$ and $V_e^D$ for frontal cortex and striatum for all subjects. $V_e^M$ was estimated from the two-compartment, three-parameter model and $V_e^D$ was estimated using the four-parameter model M1 (see text for details).

## Striatum

*Q.1. & 2.* The lack of improvement in the model fits with and without $k_5^D$, $k_7^D$ and $k_9^D$ suggest that unless these parameter values can be obtained independently (and then perhaps fixed to population averages in the model), there is no need to take into account the diffusible and non-diffusible metabolites of dopamine.

*Q.3.* The simplest mathematically justifiable model (M3) (*3*) did not yield the best AIC scores. The neglect of the known presence of significant amount of 3OMFD in plasma and brain tissue makes the physiological interpretation of the micro-parameters difficult and the model can, at best, yield a macro-parameter like $K^D = K_1k_3/k_2 + k_3$ which does not provide more information than a simple influx constant obtained from the MTGA approach ($K_i^{FD}$ versus $K^D$ has a linear correlation with $r = 0.77$, $p = 0.0011$). Indeed, from a practical standpoint, it is much simpler to generate and analyze data using the MTGA approach rather than calculating $K^D$ from individually estimated compartmental modeling parameters.

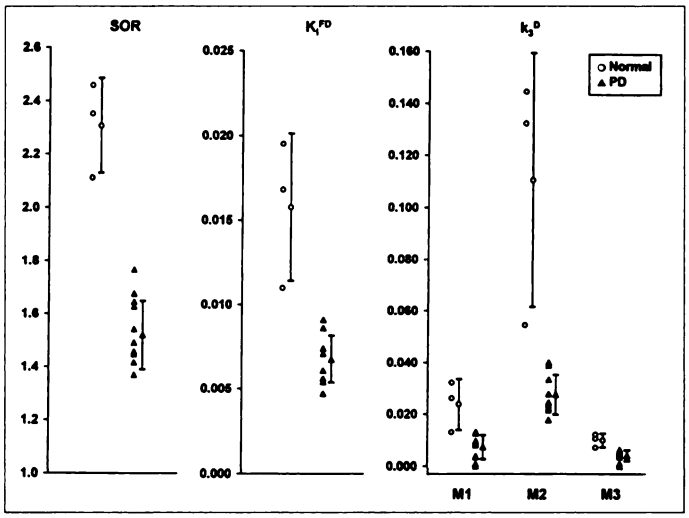


**FIGURE 6.** SOR, $K_i^{FD}$, and $k_3^D$ for normal controls and Parkinson's disease (PD) patients. Striato-occipital ratio was calculated from a 10-min scan at 90 min postinjection; $K_i^{FD}$ was estimated from the multiple time graphical approach and $k_3^D$ was estimated using three different models (M1, M2 and M3; see text for details).

*Q.4.* The difference between frontal and striatal $V_e^D$ is significant (Table 3 and Fig. 5). The model fits for striatum obtained with $V_e^D$ fixed to the frontal value had increased bias and there was no improvement in the AIC scores. This suggests that $K_1^D$ and $k_2^D$ should be fitted as independent parameters. The volumes of distribution of free FDOPA in striatum and frontal were estimated as $0.81 \pm 0.20$ and $0.66 \pm 0.13$, respectively.

*Q.5.* Higher values of q (2.3 and 1.7) have been assumed in both the M2 and M2′ models. In the M2 model, q was determined in a separate rat study (*20*) and the least squares sum criteria for different ratios of $K_1^M/K_1^D$ was used in M2′. Our data contradicts these assumed values for 3OMFD exchange across the BBB. Our $K_1^M$ and $k_2^M$ are similar to $K_1^D$ and $k_2^D$ yielding a q value of approximately 1.0. The possible species dependence of q value has recently been challenged by Cummings et al (*29*) who obtained a q value of 1.1 using kinetic analysis of previously presented rat data.

## Model Selection Criteria

In the conventional approach one determines the most appropriate model by progressively making the model more complex by adding new parameters and comparing them using the F test or AIC scores. We found, however, that because of the similarity of AIC scores for different models, one could obtain 3OMFD parameter values that were totally different from those determined by independent means. Therefore, model selection criteria should include not only WSS or AIC scores, but also biological validation: the model should yield an accurate representation of the underlying disease process. Such validation may be achieved through clinical correlations with other objective severity ratings, or discriminating minimally affected individuals from normals. Other issues require consideration in the selection of appropriate models. Often, the underlying pathophysiology is too complex to be easily modeled with a few compartments. For most PET datasets, however, nonlinear regression analysis of compartmental models cannot provide more than two or three parameters with acceptable accuracy. Additionally, increasing the number of parameters to more than four rarely improves the curve fits. These considerations invoke the need for additional assumptions in order to reduce the number of parameters to be estimated. Thus, the following question becomes critical: Should population mean parameters be substituted in complex models whenever these values can be independently obtained in separate sets of direct experiments?

Our studies suggest that the substitution of parameters from different regions may pose a problem, e.g., $V_e^D$ from frontal cortex may not apply to striatum, and that even though using $K_1^M$ and $k_2^M$ from adjunctive 3OMFD studies seems reasonable, this approach is cumbersome. Additionally, errors may result when the chosen model is sensitive to $K_1^M$ and $k_2^M$, and when the FDOPA study is performed under even minimally different conditions than those of the 3OMFD study. Population values may be used only if the model is shown to be insensitive over the range of intersubject variations in that particular parameter (*31*). Indeed, we found that model M1 does not seem to be sensitive to moderate (approximately 25%) changes in $K_1^M$ and $k_2^M$ (*30*), justifying the substitution of population mean values for individually measured parameters. Fixing $k_2^M$ to $k_2^D$ ($K_1^M/K_1^D$) and just fitting $K_1^D$, $k_3^D$ and $V_b$ does not work well, yielding bias in the last few points and increased AIC. This suggests that equal partition volume for 3OMFD and FDOPA cannot be assumed; mean striatal $V_e^M$ is approximately 10% lower than striatal $V_e^D$ (Tables 2 and 3) though the individual differences range from −57% to +25%.

Model simplifications may be implemented by pharmacolog-

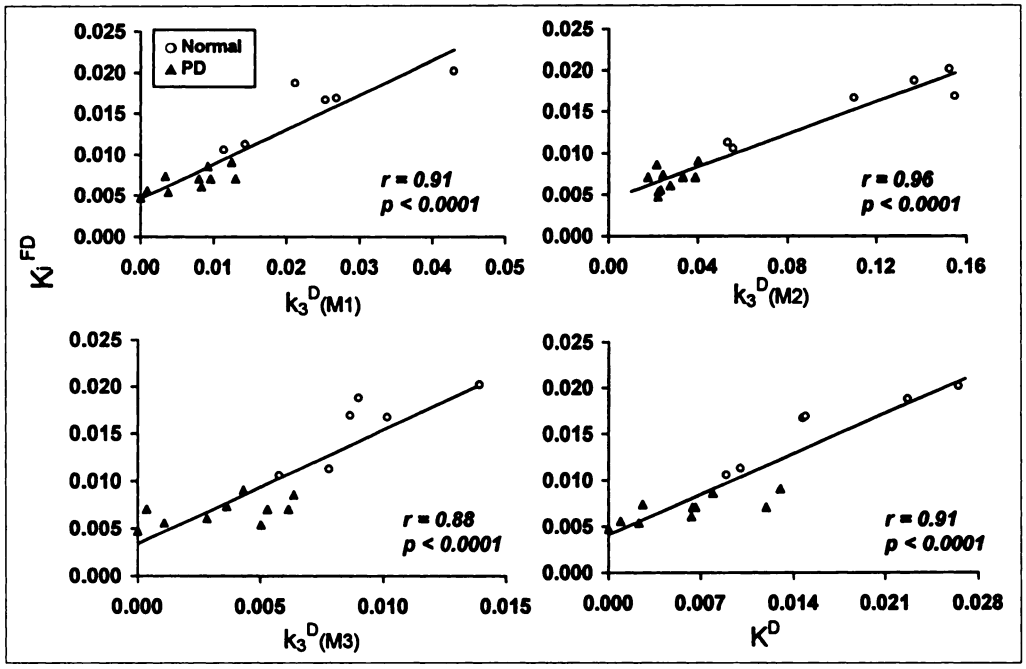


**FIGURE 7.** Correlation between $K_i^{FD}$ and the other calculated FDOPA/PET parameters. $K_D$ was calculated as $K_1k_3/k_2 + k_3$ from the microparameters obtained from model M1. Lines of linear regression through all the points are superimposed.

ical means, such as suppression of 3OMFD formation with adjunctive COMT inhibition (*32,33*). A complete supression of 3OMFD production expected with tolcapone (*34*), as opposed to a partial inhibition of 3OMFD formation with entacpone and nitecapone, may eliminate the modeling assumptions concerning 3OMFD kinetics and also simplify the PET studies by obviating the need for plasma HPLC.

### $k_3^D$ Versus Other Parameters

Discriminant analysis suggests that $K_i^{FD}$ and SOR provide the best separation of Parkinson's disease patients from normals (*26,30*). We found that $k_3^D$ parameter estimates show an interesting behavior (see Fig. 6): (a) $k_3^D$(M2) separates the two groups completely but increases the variance in the normal group, (b) $k_3^D$(M1) also separates the two groups but with relatively lower variance in the normal group and (c) $k_3^D$(M3) discriminated the two groups with similar accuracy as $k_3^D$(M1). In a larger study group, $k_3^D$(M3) did not discriminate the Parkinson's disease patients from normal controls (*30*). Thus, the choice of model may influence the outcome of critical clinical applications of the FDOPA/PET method, such as differentiating Parkinson's disease patients from normals. Moreover, in an FDOPA/PET study with a peripheral COMT inhibitor (entacapone, OR-611), we found that model choice may also affect the outcome of investigations of pharmacologic interventions. We found that with entacapone coadministration, model M2 produced a q-dependent decrease in $k_3^D$ (*32*). Model M1, which takes into account 3OMFD transport by means of average population $K_1^M$ and $k_2^M$ values produced no change in $k_3^D$ estimates with treatment, in agreement with the exclusively peripheral action of this COMT inhibitor (*35*). Thus, with model M2, estimated striatal DDC activity ($k_3^D$) can adequately discriminate Parkinson's disease patients from normals and correlate with disease severity (*30*). At the same time, however, it produces a misleading conclusion with peripheral COMT inhibition. This behavior of model M2 is probably related to the assumption of inappropriately high values for $K_1^M$ and $k_2^M$. Though we did not try explicitly to model M2′ (*1*), its behavior is expected to be similar to M2 because of the correspondingly high values it assumes for $K_1^M$ and $k_2^M$.

## CONCLUSION

The 3OMFD studies provided direct estimation of the rate constants for transport across the blood-brain barrier. The use of 3OMFD parameters in the FDOPA compartmental model allowed us to simplify the model without making assumptions that are otherwise required. The results show that striatal DDC activity estimated from a compartmental modeling approach is similar to the graphically derived unidirectional influx constant ($K_i^{FD}$) in discriminating normals from Parkinson's disease patients. This suggests that with present PET methods, clinically relevant information can be obtained from a simple graphical approach rather than a more computationally demanding compartmental technique. Most importantly, all estimated model parameters also require independent clinical validation for practical applicability in patient research. To this end, in our companion paper, we explored the strengths and weaknesses of the various FDOPA/PET modeling approaches by examining the correlation between the estimated DDC activity measures and quantitative indices of clinical disability in parkinsonism (*30*).

## ACKNOWLEDGMENTS

The authors thank Ms. Janie Dill and Ms. Jennifer Leong for help with the studies, Mr. Ralph Mattachieri and Dr. J. R. Dahl for cyclotron support and Ms. Debra Segal for manuscript preparation. This work was supported by grants from the Parkinson's Disease Foundation and the Dystonia Medical Research Foundation.

## REFERENCES

1. Huang SC, Yu DC, Barrio JR, et al. Kinetics and modeling of 6-[$^{18}$F]fluoro-L-DOPA in human PET studies. *J Cereb Blood Flow Metab* 1991;11:898–913.
2. Kuwabara H, Cumming P, Reith J, Léger G, Diksic M, Evans AC, Gjedde A. Human striatal L-DOPA decarboxylase activity estimated in vivo using 6-[$^{18}$F]fluoro-Dopa and PET: error analysis and application to normal subjects. *J Cereb Blood Flow Metab* 1993;13:57–69.
3. Wahl LM, Garnett ES, Chirakal R, et al. Quantification of dopamine metabolism in man: what is the most justifiable approach? *J Cereb Blood Flow Metab* 1993;13(suppl 1):S722.
4. Gjedde A, Reith J, Dyve S, Léger G, Guttman M, Diksic M, Evans A, Kuwabara H. DOPA decarboxylase activity of the living human brain. *Proc Natl Acad Sci* 1991;88:2721–25.
5. Patlak CS, Blasberg RG, Fenstermacher JD. Graphical evaluation of blood-to-brain transfer constants from multiple-time uptake data. *J Cereb Blood Flow Metab* 1983;3:1–7.

6. Hoehn MM, Yahr MD. Parkinsonism: onset, progression, and mortality. *Neurology* 1967;17:21–25.
7. Fahn S, Elton RL, and the UPDRS Development Committee. Unified Parkinson disease rating scale. In: Fahn S, Marsden CD, Calne D, Goldstein M, eds. *Recent developments in Parkinson's disease*, vol. 2. Floral Park, New Jersey: Macmillan; 1987:293–304.
8. Robeson W, Dhawan V, Takikawa S, et al. SuperPETT 3000 time-of-flight tomograph: optimization of factors affecting quantification. *IEEE Trans Nucl Sci* 1993;40:135–142.
9. Hariz MI, Erikson AT. Reproducibility of repeated mounting of a noninvasive CT/MRI stereoadapter. *Appl Neurophysiol* 1986;49:336–347.
10. Luxen A, Milton P, Bida GT, et al. Remote, semiautomated production of 6-[$^{18}$F]fluoro-L-dopa for human studies with PET. *Appl Radiat Isot* 1990;41:275–281.
11. Melega WP, Grafton ST, Huang SC, Satyamurthy N, Phelps ME, Barrio JR. L-6-[$^{18}$F]fluoro-DOPA metabolism in monkeys and human: biochemical parameters for the formation of tracer kinetic models with PET. *J Cereb Blood Flow Metab* 1991;11:890–897.
12. Dhawan V, Jarden JO, Strother S, Rottenberg DA. Effect of blood curve smearing on the accuracy of parameter estimates obtained for $^{82}$Rb/PET studies of blood-brain barrier permeability. *Phys Med Biol* 1988;33:61–74.
13. Eidelberg D, Takikawa S, Dhawan V, et al. Striatal $^{18}$F-DOPA uptake: absence of an aging effect. *J Cereb Blood Flow Metab* 1993;13:881–888.
14. Chaly T, Bandyopadhyay D, Matacchieri R, Belakhlef A, Dhawan V, Takikawa S, Robeson W, Margouleff D, Eidelberg D. A disposable synthetic unit for the preparation of 3-O-Methyl-6-[$^{18}$F]fluorodopa using a regioselective fluorodemercuration reaction. *J Appl Radiat Isot* 1993;45:25–30.
15. Spetsieris P, Dhawan V, Takikawa S, Margouleff D, Eidelberg D. A versatile graphics-image processing package for imaging cerebral function. *IEEE Computer Graphics and Applications* 1993;13:15–26.
16. Talairach J, Tournoux P. *Co-planar stereotaxic atlas of the human brain.* New York: Thieme Medical Publishers, Inc., 1988.
17. Doudet DJ, McLellan CA, Carson R, et al. Distribution and kinetics of 3-O methyl-6-[$^{18}$F]fluoro-L-DOPA in the rhesus monkey brain. *J Cereb Blood Flow Metab* 1991;11:726–734.
18. Wahl LM, Chirakal R, Firnau, et al. The distribution and kinetics of [$^{18}$F]6-Fluoro-3-O methyl-L-dopa in the human brain. *J Cereb Blood Flow Metab* 1993;14:664–670.
19. Firnau G, Sood S, Chirakal R, Nahmias C, Garnett S. Cerebral metabolism of 6-[$^{18}$F]fluoro-L-3,4-Dihydroxyphenylalanine in the primate. *J Neurochem* 1987;29: 1077–82.
20. Reith J, Dyve S, Kuwabara H, Guttman M, Diksic M, Gjedde A. Blood-brain transfer and metabolism of 6-[$^{18}$F]fluoro-L-Dopa in rat. *J Cereb Blood Flow Metab* 1990;10: 707–719.
21. Akaike A. Posterior probabilities for choosing a regression model. *Ann Inst Math Sci* 1978;30:9–14.
22. Patlak CS, Dhawan V, Takikawa S, et al. Estimation of striatal uptake rate constant of FDOPA using PET: methodological issues. *Ann Nucl Med* 1993;7(suppl):S46–S47.
23. Hoshi H, Kuwabara H, Léger G, Cumming P, Guttman M, Gjedde A. 6-[$^{18}$F]fluoro-L-Dopa metabolism in living human brain: a comparison of six analytical methods. *J Cereb Blood Flow Metab* 1993;13:57–69.
24. Anderson TW. *An introduction to multivariate statistical analysis.* New York: John Wiley & Sons; 1984.
25. Takikawa S, Dhawan V, Chaly T, et al. Input functions for 6-[fluorine-18]fluorodopa quantitation in parkinsonism: comparative studies and clinical correlations. *J Nucl Med* 1994;35:955–963.
26. Firnau G, Sood S, Chirakal R, Nahmias C, Garnett S. Metabolites of 6-[$^{18}$F]fluoro-L-Dopa in human blood. *J Nucl Med* 1988;29:363–369.
27. Eidelberg D, Moeller JR, Dhawan V, et al. The metabolic anatomy of Parkinson's disease: complementary [$^{18}$F]fluorodeoxyglucose and [$^{18}$F]fluorodopa positron emission tomographic studies. *Mov Disorders* 1990;5:203–213.
28. Koeppe R, Mangner T, Betz AL, et al. Use of [$^{11}$C]aminocyclohexanecarboxylate for the measurement of amino acid uptake and distribution volume in human brain. *J Cereb Blood Flow Metab* 1990;10:727–739.
29. Cumming P, Kuwabara H, Gjedde A. A kinetic analysis of 6-[$^{18}$F]fluoro-L-Dihydroxyphenylalanine metabolism in the rat. *J Neurochem* 1994;63:1675–1682.
30. Ishikawa T, Dhawan V, Chaly T, et al. Clinical significance of striatal DOPA decarboxylase activity in Parkinson's disease. *J Nucl Med* 1996;37:216–222.
31. Carson RE, Doudet DJ, McLellan, et al. Combined modeling analysis of 6-[F-18]fluoro-L-dopa (FDOPA) and 3-O-methyl-6-[F-18]fluoro-l-dopa (OMFD) in non-human primates. *J Nucl Med* 1992;33:945.
32. Ishikawa T, Dhawan V, Chaly T, et al. [$^{18}$F]fluoro-L-dopa (FDOPA/PET) with an inhibitor of catechol-O-methyltransferase: effect of the plasma 3-O-methyldopa fraction on data analysis [Abstract]. *J Nucl Med* 1995;36(suppl):186P.
33. Laihinen A, Rinne JO, Rinne UK, et al. [$^{18}$F]-6-Fluorodopa PET scanning in Parkinson's disease after selective COMT inhibition with nitecapone (OR-462). *Neurol* 1992;42:199–203.
34. Gunther I, Psylla M, Antonini, et al. [$^{18}$F]Fluoro-L-dopa (FD) uptake and arterial plasma tracer metabolite alterations as a result of catechol-O-methyl transferase (COMT) and L-aromatic-amino-acid-decarboxylase (AAAD). *Neurology* 1993;43: A196.
35. Mannisto PT, Tuomainen P, Tuominen RK. Different in vivo properties of three new inhibitors of catechol O-methyltransferase in the rat. *Br J Pharmacol* 1992;105:569–574.

# Clinical Significance of Striatal DOPA Decarboxylase Activity in Parkinson's Disease

Tatsuya Ishikawa, Vijay Dhawan, Thomas Chaly, Claude Margouleff, William Robeson, J. Robert Dahl, Francine Mandel, Phoebe Spetsieris and David Eidelberg

*The Departments of Neurology, Research, Medicine and Biostatistics, North Shore University Hospital/Cornell University Medical College, Manhasset, New York*

We performed dynamic PET studies with fluorodopa (FDOPA) in 9 normal volunteers and 16 patients with Parkinson's disease to investigate the applicability of dopa decarboxylase (DDC) activity measurements as useful markers of the parkinsonian disease process. **Methods:** From the 3-O-methyl-FDOPA (3OMFD)/PET studies, we obtained mean population values of the kinetic rate constants for 3OMFD ($K_1^M$ = 0.0400 and $k_2^M$ = 0.0420). We applied these values to calculate striatal DDC activity using the FDOPA compartmental model. We estimated $k_3^D$ in this group using dynamic FDOPA-PET and population mean $K_1^M$ and $k_2^M$ values. We then applied the mean population $K_1^M$ and $k_2^M$ values to estimate $k_3^D$(pop) to a new group (6 normal volunteers and 11 patients) studied only with dynamic FDOPA-PET. In all FDOPA/PET studies, we calculated striatal uptake rate constants ($K_i^{FD}$) using a graphical method and also measured the striato-occipital ratio (SOR). **Results:** Although DDC activity has been postulated as a precise indicator of presynaptic nigrostriatal dopaminergic function, $K_i^{FD}$ and SOR provided better between-group discrimination than did estimates of striatal DDC activity. $K_i^{FD}$ and $k_3^D$(pop) both correlated significantly with quantitative disease severity ratings, with a similar degree of accuracy ($r$ = 0.69 and 0.63 for $k_3^D$(pop) and $K_i^{FD}$, respectively; $p < 0.01$). **Conclusion:** Although estimated striatal DDC activity correlates with clinical disability, this measure is comparably less effective for early diagnosis. We conclude that a simple estimate such as striatal $K_i^{FD}$ is superior to $k_3^D$ measurements for most clinical and research applications.

**Key Words:** DOPA decarboxylase activity; PET; parkinsonism

**J Nucl Med 1996; 37:216–222**

Parkinson's disease is characterized by presynaptic nigrostriatal dopamine dysfunction. PET and 6-[$^{18}$F]fluoro-L-dopa (FDOPA) have been used to assess the presynaptic nigrostriatal dopaminergic function in life, to provide an objective measure of disease severity in Parkinson's disease patients and to

Received Nov. 28, 1994; revision accepted Jun. 26, 1995.

For correspondence or reprints contact: David Eidelberg, MD, Department of Neurology, North Shore University Hospital/Cornell University Medical College, 300 Community Dr., Manhasset, NY 11030.